IEEE Access
Multidisciplinary | Rapid Review | Open Access Journal

IEEE BROADCAST TECHNOLOGY SOCIETY SECTION

Received 11 May 2022, accepted 27 June 2022, date of publication 5 July 2022, date of current version 27 July 2022.

Digital Object Identifier 10.1109/ACCESS.2022.3188675

RESEARCH ARTICLE

Novel PAPR Reduction Algorithms for OFDM Signals

QUANG NGUYEN, THE KHAI NGUYEN, HA H. NGUYEN, (Senior Member, IEEE), AND BRIAN BERSCHEID, (Member, IEEE)

Department of Electrical and Computer Engineering, University of Saskatchewan, Saskatoon, SK S7N 5A9, Canada

Corresponding author: Ha H. Nguyen (ha.nguyen@usask.ca)

This work was supported by the Vecima Networks and Natural Sciences and Engineering Research Council of Canada (NSERC) under a Collaborative Research Development (CRD) Grant.

ABSTRACT This paper proposes two efficient peak-to-average power ratio (PAPR) reduction algorithms for OFDM signals based on the principle of tone reservation. The first algorithm is performed in the time domain, whereas the second algorithm is a new clipping-and-filtering method. Both algorithms consist of two stages. The first stage, which is done off-line, precomputes a set of canceling signals based on the settings of the OFDM system. In particular, these signals are constructed to cancel signals at different levels of maximum instantaneous power that are above a predefined threshold. The second stage, which is online and iterative, reduces the signal peaks using modified versions of the canceling signals constructed in the first stage. When the reserved tones are distributed among the data tones, analysis and simulation results obtained with Data Over Cable Service Interface Specifications (DOCSIS) parameters show that the proposed algorithms achieve slightly better PAPR reduction performance and with significantly lower complexity when compared to the conventional algorithms.

INDEX TERMS Clipping-and-filtering (CF), clipping noise, DOCSIS, OFDM, PAPR, tone reservation.

I. INTRODUCTION

Data Over Cable Service Interface Specifications (DOCSIS) is an industry standard for data communications over cables and it has been playing an increasingly important role in shaping the next generation of cable networks. Due to the high demand on video streaming applications in the recent years, the needs to improve connectivity, data rates and quality services have become more and more pressing. The physical layer in the current DOCSIS standard still relies on orthogonal frequency division multiplexing (OFDM) to provide up to 10 Gbps downstream and 1 Gbps upstream. A major drawback of OFDM that limits its performance is the high peak-to-average power ratio (PAPR). This is because high-PAPR signals require a linear high-power amplifier (HPA), which is usually very inefficient. Moreover, given the limited linear range of an HPA, the high-PAPR signals are occasionally approach the saturation region of the amplifier, causing large in-band and out-of-band distortions.

The associate editor coordinating the review of this manuscript and approving it for publication was Jian Song.

Over the years, various techniques have been developed to reduce the peak of an OFDM signal, such as clipping and filtering, tone reservation (TR), multiple signaling and coding [1]. The coding approaches embed the data sequence in a longer sequence and only a subset of all possible sequences is used to exclude patterns with high PAPR. The multiple signaling schemes reduce the peak of a signal by controlling the phase of the data sequence through a phase optimization process.

Clipping and filtering is probably the simplest method but it distorts the desired in-band signal, resulting in bit-error-rate (BER) degradation and also increases adjacent out-of-band distortion [2]. These distortions might not be accepted in many practical OFDM systems where the amount of in-band distortion is highly restricted due to the use of very high order QAM modulation.

The TR approach was first proposed in [3], which reserves a number of subcarriers to generate a peak canceling signal that can reduce the peak power of the transmitted signal. The subcarriers or tones are selected to be mutually exclusive with the tones used for data transmission, which allows

the receiver to extract the data symbols without distortion. Although this approach can achieve effective cancellation, the search for an appropriate cancellation signal involves high computational complexity. Specifically, gradient-based search methods have been shown to achieve good results [4], but with relatively high complexity. The gradient method tries to reduce the peaks of OFDM signals within a predefined threshold in an iterative manner. However, its convergence rate is slow and the number of multiplications and additions performed per iteration can be high. Thus, many schemes has been proposed to achieve faster convergence and/or lower computational complexity. The authors in [5] apply a cross-entropy method to search for a suboptimal reserved tone set to achieve a higher peak reduction per iteration. In [6], [7], the authors propose different techniques to jointly optimize the clipping threshold along with the peak-canceling signals.

Moreover, tone reservation can also be combined with the technique of clipping and filtering to provide a different method for PAPR reduction, which shall be called clipping-and-filtering TR (CFTR) [8]. This method takes advantage of the computational efficiencies of the FFT/IFFT algorithms and processes signals in the frequency domain instead of the time domain. A drawback of the CFTR method is that a large number of iterations is usually required to obtain the desired amount of peak reduction. The authors in [9] apply convex optimization to find the optimal filters to reduce the number of iterations. A faster convergence speed can also be achieved by applying a suitable scaling factor to the filtered signal, which was investigated in [10]–[12].

In general, all the PAPR reduction methods discussed above entail significant complexity and overhead when reducing signal peaks online. In particular, the complexity of finding the optimal solution for a general case with the TR algorithm could become prohibitive for a wideband system with a large number of subcarriers [13], such as in DOCSIS when the number of subcarriers could be as high as 8,192. Furthermore, in certain applications, the number of subcarriers along with their tone locations might change over time, which makes it harder to find a suitable peak reduction signal in a small number of iterations.

To deal with the high complexity issue, the authors in [14] utilize feed-forward neural networks to generate a pre-generated set of canceling signals for PAPR reduction, which promises a linear complexity order. However, the complexity of the method in [14] is also proportional to the number of hidden layers, which is in the order of hundreds, and hence still be computationally demanding. In [15], a novel method of solving the clipping and filtering problem in the time domain is presented that has a lower computational complexity when compared to the conventional CFTR method. However, the applicability of the method in [15] to cable systems is very limited. This is because the reported results on error vector magnitude and modulation error rate are in the range of 20 dB, which is far less than what required for high-order constellations (as large as 4,096 QAM constellation) employed in DOCSIS. Moreover, the method in [15] causes distortion to the data tones, which is evidenced by the degraded BER performance presented in [15]. Another TR method was recently proposed in [16] that is based on parallel Tabu search to find a sub-optimal peak reduction tone set. The sub-optimal peak reduction tone set in then used together with adaptive iterative clipping and filtering. However, like the method in [15], the method in [16] also introduces distortion to the data tones, which degrades the BER.

This paper builds upon the clipping noise analysis presented in [17] and proposes two efficient PAPR reduction algorithms that are specifically suitable for DOCSIS networks. Both algorithms consist of two stages. The first stage is done off-line (i.e., not in real time and independent of the transmitted OFDM signals) to precompute a set of cancellation signals. The second stage is performed online (i.e., in real time and based on the actual transmitted OFDM signals) and in an iterative manner to reduce the peaks of OFDM symbols by performing simple transformations upon the precomputed cancellation signals. Simulation results show that the proposed algorithms can obtain very good peak reduction with a smaller number of iterations, and with fewer numbers of multiplications and additions per iteration when compared to the conventional TR and CFTR algorithms. It is stressed that both the proposed PAPR reduction algorithms are distortionless, which means that they do not affect the BER of the information bits sent over the data tones. As such, the proposed algorithms could greatly facilitate the implementation of future wideband OFDM-based communication systems, such as those used in high-speed wireless or broadband cable systems.

The remainder of this paper is organized as follows. Section II reviews OFDM signals. Section III discusses conventional peak reduction algorithms. Section IV describes the algorithms proposed in this paper. Section V analyzes and compare computational complexities of different PAPR reduction methods. Simulations results are given in Section VI. Section VII concludes the paper.

II. OFDM SIGNALS

In an OFDM system, N data symbols $X_0, \ldots, X_{N-1}$ are modulated on a set of N orthogonal subcarriers. The analog baseband-equivalent form of an OFDM symbol is:

$$x(t) = \frac{1}{\sqrt{N}} \sum_{k=0}^{N-1} X_k e^{j\frac{2\pi k}{T}t}, \quad 0 \le t \le T, \tag{1}$$

where T is the symbol duration and $\Delta f = 1/T$ is the frequency spacing between adjacent subcarriers.

A discrete-time OFDM signal $\boldsymbol{x} = [x[0], \ldots, x[NJ-1]]$ is obtained by sampling $x(t)$ with the sampling frequency $F_s = NJ/T$, where J denotes the oversampling factor. That is:

$$x[n] = x(t)|_{t=\frac{nT}{JN}} = \frac{1}{\sqrt{N}} \sum_{k=0}^{N-1} X_k e^{j2\pi\frac{nk}{NJ}}, \quad 0 \le n \le NJ-1, \tag{2}$$

The oversampled discrete-time signal in (2) can be produced by padding $(J-1)N$ zero values in the middle of the frequency symbol and performing a JN-length IFFT operation on the padded frequency symbol. The padded frequency symbol is:

$$\boldsymbol{X} = \big[X_0, \ldots, X_{N/2-1}, \underbrace{0, \ldots, 0}_{(J-1)N \text{zeros}}, X_{N/2}, \ldots, X_{N-1}\big]. \quad (3)$$

The PAPR of the analog OFDM signal $x(t)$ is defined in a symbol-wise manner as

$$\text{PAPR}_\text{C}(x) = \frac{\max_{0\le t\le T}|x(t)|^2}{E\{|x(t)|^2\}}. \quad (4)$$

A measurement of PAPR using discrete time samples is:

$$\text{PAPR}_\text{D}(x) = \frac{\max_{0\le n\le NJ-1}|x[n]|^2}{E\{|x[n]|^2\}}. \quad (5)$$

In order to have (5) approximate well the PAPR of the analog signal given by (4), it is required that $J \ge 4$ [18].

In the literature, it is customary to use the complimentary cumulative distribution function (CCDF) of the PAPR as a performance criterion, which is defined as:

$$\text{CCDF}(\psi) = \Pr\{\text{PAPR}_\text{D}(x) \ge \psi\}. \quad (6)$$

If N is large enough ($N \ge 64$ is practically sufficient), then based on the central limit theorem, the real and imaginary parts of $x[n]$ have Gaussian distributions, hence the envelope of $x[n]$ follows a Rayleigh distribution [1]. Also, in theory, the maximum possible PAPR, which occurs when all subcarriers align in phase, is proportional to the number of active subcarriers.

III. OVERVIEW OF TR TECHNIQUES

In TR techniques, both the transmitter and the receiver must agree to reserve a set of G subcarriers for peak reduction, while the remaining $(N-G)$ subcarriers are used for data transmission. Peak canceling signal $\boldsymbol{c} = [c[0], \ldots, c[NJ-1]]$ is constructed from the reserved tones. The peak-reduced signal $\boldsymbol{y} = [y[0], \ldots, y[NJ-1]]$ is given by:

$$y[n] = x[n] + c[n] = \frac{1}{\sqrt{N}}\sum_{k=0}^{N-1}(X_k + C_k)e^{j2\pi\frac{nk}{NJ}}, \quad (7)$$

where $0 \le n \le NJ-1$ and

$$\boldsymbol{C} = \big[C_0, \ldots, C_{N/2-1}, 0, \ldots, 0, C_{N/2}, \ldots, C_{N-1}\big]^T$$

is the frequency symbol used to construct $\boldsymbol{c}$.

The set of subcarriers used is referred to as a peak reservation tone set (PRT), denoted as $\mathcal{R} = \{i_0, i_1, \ldots, i_{G-1}\}$. The frequency vector $\boldsymbol{C}$ is restricted to have non-zero elements only at the reserved tones. That is:

$$X_k + C_k = \begin{cases} X_k, & k \in \mathcal{D} \\ C_k, & k \in \mathcal{R} \end{cases}, \quad (8)$$

where $\mathcal{D}$ is the set of data tones, and $\mathcal{D} \cap \mathcal{R} = \emptyset$.

The PAPR of the peak-reduced OFDM signal is then computed as [4]

$$\text{PAPR}(y) = \frac{\max_{0\le n\le NJ-1}|x[n]+c[n]|^2}{E\{|x[n]|^2\}}. \quad (9)$$

Since the denominator of (9) does not depend on $\boldsymbol{C}$, the optimal peak canceling signal is chosen to minimize the peak power of $y[n]$:

$$\boldsymbol{C} = \arg\min_{\boldsymbol{C}\in\mathbb{C}^N}\left\{\max_{0\le n\le NJ-1}|x[n]+c[n]|^2\right\}, \quad \text{subject to: } \mathcal{H}(\boldsymbol{C}) \le G \quad (10)$$

where $\mathbb{C}^N$ is the N-dimensional complex number space and $\mathcal{H}(\boldsymbol{v})$ denotes the Hamming weight of vector $\boldsymbol{v}$, which is the number of non-zero elements in $\boldsymbol{v}$.

The problem in (10) can be expressed in the form of quadratic programming [19]. The optimum solution can be found but it requires high computational cost, which is not suitable for online processing. Instead of solving for the optimal canceling signal, one could find a canceling signal to bring the peak of $y[n]$ to be very close to some predefined threshold, $\mathcal{T}$. This is explained further below.

Given a threshold $\mathcal{T}$, introduce a clipping function [3]:

$$g_\mathcal{T}(\xi) = \begin{cases} \xi, & \text{if } |\xi| \le \mathcal{T} \\ \mathcal{T}\, e^{j\angle\xi}, & \text{if } |\xi| > \mathcal{T}, \end{cases} \quad (11)$$

where ξ is a complex variable. By applying the clipping function to $y[n]$, the problem in (10) is transformed into the following problem:

$$\boldsymbol{C} = \arg\min_{\boldsymbol{C}\in\mathbb{C}^G}\left\{\sum_{n=0}^{NJ-1}|x[n]+c[n]-g_\mathcal{T}(x[n]+c[n])|^2\right\}, \quad \text{subject to: } \mathcal{H}(\boldsymbol{C}) \le G \quad (12)$$

Let $\boldsymbol{f} = [f[0], \ldots, f[NJ-1]]$ be the residual signal after applying the clipping operation on $y[n]$. That is,

$$f[n] = y[n] - g_\mathcal{T}(y[n]). \quad (13)$$

The optimization problem in (12) tries to find $\boldsymbol{c}$ to minimize the power of $\boldsymbol{f}$. For this reason, $\boldsymbol{f}$ is also called the *clipping noise* associated with the signal $\boldsymbol{y}$, and the optimum $\boldsymbol{c}$ helps to create a signal with minimal level of this noise.

A. CONVENTIONAL GRADIENT-BASED TR (GTR) ALGORITHM

The gradient algorithm in [3] solves the problem in (12) in an iterative manner as follows. At the kth step of the algorithm:

$$\boldsymbol{c}_{k+1} = \boldsymbol{c}_k - \gamma\sum_{i\in\mathcal{M}_k}\alpha_{k,i}\circlearrowleft_i(\boldsymbol{k}), \quad (14)$$

where γ is a constant; $\mathcal{M}_k$ is the set of indices of those samples in $(\boldsymbol{x}+\boldsymbol{c}_k)$ having their magnitudes larger than $\mathcal{T}$; $\boldsymbol{k} = [k[0], \ldots, k[NJ-1]]$ is called a *kernel*, which is obtained by setting the magnitudes of the reserved tones to 1 and then

performing an Inverse Discrete Fourier Transform (IDFT). That is:

$$k[n] = \frac{1}{|\mathcal{R}|} \sum_{\ell=0}^{NJ-1} p[\ell] \mathrm{e}^{j2\pi \frac{n\ell}{NJ}}, \; 0 \le n \le NJ-1, \tag{15}$$

where

$$p[\ell] = \begin{cases} 1, & \text{if } \ell \in \mathcal{R} \\ 0, & \text{otherwise} \end{cases}.$$

The operation $\circlearrowleft_i(\boldsymbol{v})$ represents a circular shift of a time vector $\boldsymbol{v}$ by i samples to the right, whereas $\alpha_{k,i}$ is a complex value given by:

$$\alpha_{k,i} = (|x[i] + c_k[i]| - \mathcal{T})\, \mathrm{e}^{j\angle(x[i]+c_k[i])}. \tag{16}$$

The resulting signal after performing k iterations is:

$$\boldsymbol{y}_k = \boldsymbol{x} + \boldsymbol{c}_k. \tag{17}$$

The process stops when either a maximum number of iterations is reached or no peak above $\mathcal{T}$ in $\boldsymbol{y}_k$ is found, i.e., $\max |\boldsymbol{y}_k| < \mathcal{T}$.

B. CONVENTIONAL CLIPPING AND FILTERING TR (CFTR) ALGORITHM

The high complexity of the GTR algorithm could be reduced by first performing clipping, then filtering the clipping noise defined in (13). The clipping operation, however, causes distortions to the data tones. Thus, filtering is implemented so that only the frequency portion of the clipping noise that corresponds to locations of the reserved tones is retained. That is, the filter is defined as:

$$H(\mathrm{e}^{j\omega}) = \begin{cases} 1, & \text{if } \omega \in \mathcal{R} \\ 0, & \text{otherwise} \end{cases}. \tag{18}$$

In other words, the filtering operation in (18) is simply a projection on the reserved tone set. Hence, a signal obtained after filtering the clipping noise is:

$$\boldsymbol{c} = \mathcal{F}^{-1}\left\{H\left(\mathcal{F}\{\boldsymbol{f}\}\right)\right\}, \tag{19}$$

where $\mathcal{F}$ denotes the discrete Fourier transform (DFT) and $\mathcal{F}^{-1}$ is the inverse DFT (IDFT). The canceling vector $\boldsymbol{c}$ is then scaled by a factor β to further suppress the peak of the resulting signal [10], [11]. That is,

$$\hat{\boldsymbol{y}} = \boldsymbol{y} + \beta \boldsymbol{c}. \tag{20}$$

The factor β is chosen to minimize the mean squared error between the canceling signal and clipping noise:

$$\beta = \arg\min_{\beta} \sum_{n \in \mathcal{S}} |f[n] - \beta c[n]|^2, \tag{21}$$

where $\mathcal{S}$ represents the set of the peak samples. There are two methods of selecting this set, which are proposed in [10] and [11]. In this paper, the set is defined as in [10], which is $\mathcal{S} = \{n : |x[n]| > \mathcal{T}\}$. This set resembles the set $\mathcal{M}_k$ used in the GTR algorithm discussed previously. A solution to the problem in (21) is given by

$$\beta = \frac{\Re\left[\sum_{n \in \mathcal{S}} f[n] c^*[n]\right]}{\sum_{n \in \mathcal{S}} |c[n]|^2}, \tag{22}$$

where $c^*[n]$ is a complex conjugate of $c[n]$. It is pointed out that, due to the effect of the filter $H(\mathrm{e}^{j\omega})$, the peak regrows significantly. As a consequence, multiple iterations of the clipping and filtering are required to obtain satisfactory PAPR reduction. The algorithm is illustrated in Fig. 1.

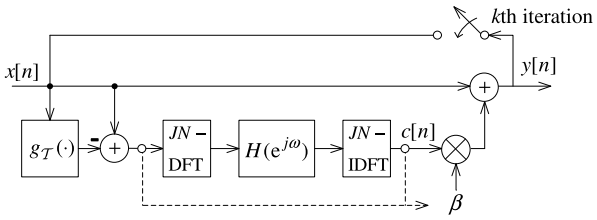

FIGURE 1. Conventional clipping and filtering TR algorithm.

IV. PROPOSED ALGORITHMS

Two novel PAPR reduction algorithms are proposed in this paper. The first algorithm works in the time-domain, aiming to improve the performance of the GTR algorithm. The second algorithm is performed in the frequency-domain to reduce the complexity of the CFTR algorithm.

A. PROPOSED TIME-DOMAIN ALGORITHM

The main idea of the proposed time-domain algorithm is to create a database of canceling signals for different levels of peak magnitudes, then reuse them to reduce the peaks of symbols having the same magnitudes. This is done in two stages. The first stage is called a learning stage, which initializes a set of peak reduction signals corresponding to the clipping noise of different maximum magnitudes. This stage can be done off-line and updated regularly when needed. The second stage is an online process, which combines the conventional TR and some pre-processing steps using the canceling signals developed in the first stage.

Provided that $\mathcal{T}$ is large enough, the authors in [17] show that the clipping noise defined in (13) can be approximated by a sum of constant-phase parabolic pulses, with each pulse having one local minimum or maximum. As an example, Fig. 2 plots a symbol having one dominant peak above $\mathcal{T}$ and its corresponding clipping noise. In order to effectively reduce this peak, the most effective signal $\boldsymbol{c}$ should be the one that closely resembles the inverse of the clipping pulse. Due to the property of having a nearly constant phase around the over-threshold samples, the signal $\boldsymbol{c}$ can be reused to cancel other clipping pulses with the same peak magnitude by cyclic-shifting it to align in time with the pulse and phase shifting it to align with the complex phase of the pulse. Since

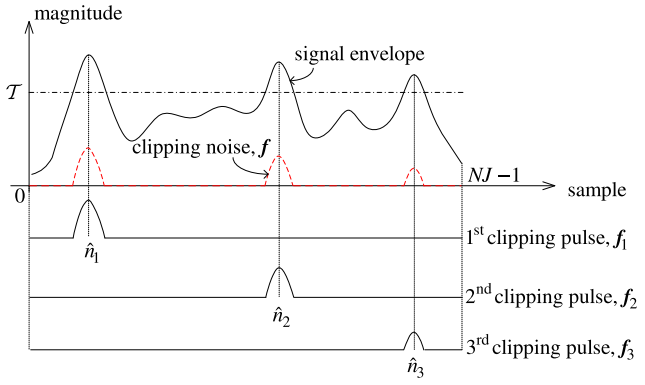

FIGURE 2. Example of clipping noise and clipping pulses.

cyclic-shifting a signal in the time domain and performing a phase rotation does not change its frequency components, the newly shifted time signal still contains only those tones which are reserved for peak reduction.

1) STAGE 1 – LEARNING

Given $\mathcal{T}$, a set of possible levels of peak magnitude is formed as:

$$\mathcal{L}_{\mathcal{T}} = \left\{\mathcal{T}_i = \mathcal{T} + i\delta_{\mathcal{T}},\ 1 \le i \le q,\ \delta_{\mathcal{T}} > 0\right\}, \tag{23}$$

where $\delta_{\mathcal{T}}$ is the step size and $\mathcal{T}_q$ is the maximum peak amplitude. A large number of randomized OFDM symbols is then generated and their peak amplitudes are recorded and classified into q sets:

$$\mathcal{B}_i = \{\boldsymbol{x} : \mathcal{T}_i \le \max|\boldsymbol{x}| \le \mathcal{T}_{i+1}\},\ i = 1, \ldots, q. \tag{24}$$

For each set in (24), a reference signal is constructed as:

$$\hat{\boldsymbol{x}}_i = \frac{1}{|\mathcal{B}_i|} \sum_{\boldsymbol{x}\in\mathcal{B}_i} \circlearrowleft_{-\hat{n}} \left(\boldsymbol{x}\, \mathrm{e}^{-j\angle x[\hat{n}]}\right), \tag{25}$$

where $x[\hat{n}]$ is the sample of $\boldsymbol{x}$ having the maximum magnitude. The reference signal in (25) is obtained in three steps. The first step cancels the phase of the highest peak sample. Second, the time samples are cyclically shifted to the original time index. After this, the OFDM symbols in $\mathcal{B}_i$ are all aligned at 0 index, with roughly zero phase for samples around the zero index, and uncorrelated phases for other samples. This causes their sum in the third step to have a high ratio between its major lobe and side lobes. Moreover, the reference signal still has the same frequency tones as the OFDM symbols since averaging and phase shifting do not introduce any new frequency content.

For each reference signal, the corresponding peak canceling signal is found to reduce its peak below $\mathcal{T}$. This can be achieved by applying the conventional TR technique to produce:

$$\hat{\boldsymbol{c}}_{\mathcal{T},i} \leftarrow \mathrm{TR}\left(\hat{\boldsymbol{x}}_i, \boldsymbol{k}, \mathcal{T}\right). \tag{26}$$

The first stage finishes by finding a set of peak canceling signals

$$\mathcal{C}_{\mathcal{T}} = \left\{\hat{\boldsymbol{c}}_{\mathcal{T},1}, \ldots, \hat{\boldsymbol{c}}_{\mathcal{T},q}\right\}. \tag{27}$$

2) STAGE 2 – Peak-Reduction LOOP

The second stage reduces the peak for each OFDM symbol iteratively. At the kth step of the algorithm, the residual signal vector $\boldsymbol{f}_k = \boldsymbol{x} + \boldsymbol{c}_k - g_{\mathcal{T}}(\boldsymbol{x} + \boldsymbol{c}_k)$ is approximated by P_k clipping pulses:

$$\boldsymbol{f}_k \approx \sum_{i=1}^{P_k} \boldsymbol{f}_{k,i}, \tag{28}$$

where $\boldsymbol{f}_{k,i}$ is the ith pulse. Each clipping pulse has a maximum peak magnitude sample, which is the set of peak samples in $\boldsymbol{f}_k$ (see Fig. 2):

$$\mathfrak{P}_k = \left\{\hat{n} : |f_k[\hat{n}]| \ge \max\left(|f_k[\hat{n}-1]|, |f_k[\hat{n}+1]|\right)\right\}. \tag{29}$$

The number of clipping pulses is equal to the number of elements in this set, that is $|\mathfrak{P}_k| = P_k$. For each clipping pulse $\boldsymbol{f}_{k,i}$, which has the peak magnitude sample at $\hat{n}_i \in \mathfrak{P}_k$, a corresponding level index of the ith pulse is found by:

$$\ell_{k,i} = \min\left(\left\lfloor \frac{\max|\boldsymbol{f}_{k,i}|}{\delta_{\mathcal{T}}} \right\rfloor, q\right). \tag{30}$$

Since

$$\max|\boldsymbol{f}_{k,i}| = |f_{k,i}[\hat{n}_i]| = |f_k[\hat{n}_i]|,$$

equation (30) can be simplified to:

$$\ell_{k,i} = \min\left(\left\lfloor \frac{|f_k[\hat{n}_i]|}{\delta_{\mathcal{T}}} \right\rfloor, q\right). \tag{31}$$

Then, a canceling pulse for $\boldsymbol{f}_{k,i}$ is obtained by:

$$\hat{\boldsymbol{f}}_{k,i} = \circlearrowleft_{\hat{n}_i} \left(\hat{\boldsymbol{c}}_{\mathcal{T},\ell_{k,i}}\, \mathrm{e}^{+j\angle f_{k,i}[\hat{n}_i]}\right) \approx \boldsymbol{f}_{k,i}. \tag{32}$$

The overall canceling signal is then constructed by combining the individual canceling pulses:

$$\boldsymbol{c}_{k+1} = \boldsymbol{c}_k - \sum_{i=1}^{P_k} \hat{\boldsymbol{f}}_{k,i}. \tag{33}$$

The process repeats until either a maximum number of iterations is reached or all the samples in the peak-reduced signal vector are below the threshold $\mathcal{T}$.

In summary, the proposed algorithm is outlined below.

Learning Stage

1) Input: Kernel vector $\boldsymbol{k}$; threshold $\mathcal{T}$; set $\mathcal{D}$; set $\mathcal{R}$
2) Initialization:
   - Initialize q, resolution $\delta_{\mathcal{T}}$, set $\mathcal{L}_{\mathcal{T}}$ as in (23)
   - Initialize q sets $\mathcal{B}_1 = \ldots = \mathcal{B}_q = \emptyset$
   - Randomly generate a large number of OFDM symbols with data tones $\mathcal{D}$.
3) Learning:
   a) Classify OFDM symbols into q sets as in (24)

b) Generate reference signals, and their canceling signals using (25), (26).
c) After all symbols have been processed, Return $\mathcal{C}_{\mathcal{T}}$

Peak-Reduction Stage

1) Input: Symbol vector $\boldsymbol{x}$; Kernel vector $\boldsymbol{k}$; Threshold $\mathcal{T}$; Number of iterations N_{it}; Canceling signal set $\mathcal{C}_{\mathcal{T}}$
2) Initialization: Loop variable $k = 1$; $\boldsymbol{c}_k = 0$;
3) Loop_Begin:
   - Determine set of peak samples in clipping noise using (29)
   - Calculate $\boldsymbol{c}_{k+1}$ using (31), (32) and (33)
4) Loop_End:
   - If $(k > N_{\text{it}})$ return $\boldsymbol{y}_{k+1} = \boldsymbol{c}_{k+1} + \boldsymbol{x}$
   - Else $k = k + 1$, jump Loop_Begin

B. PROPOSED CLIPPING AND FILTERING ALGORITHM

This section proposes a new clipping and filtering algorithm, which uses precalculated canceling signals. In contrast to the conventional CFTR algorithm, which applies unity gain to each reserved tone via $H(\mathrm{e}^{j\omega})$ in (18), the proposed algorithm establishes an individual gain for each reserved tone. This algorithm has two stages. The first stage calculates the gain coefficients off-line. The second stage is an online process, which iteratively reduces the peak using the precomputed gains.

Recall that the clipping noise $\boldsymbol{f}$ in (13) can be approximated by a sum of P_k clipping pulses as $\boldsymbol{f} = \sum_{i=1}^{P_k} \boldsymbol{f}_i$, where $\boldsymbol{f}_i$ is the ith clipping pulse with its maximum amplitude at $\hat{n}_i$. Then the peak canceling signal can be constructed as a combination of the canceling pulses:

$$\boldsymbol{c} = \sum_{i=1}^{P_k} \boldsymbol{c}_i, \tag{34}$$

where $\boldsymbol{c}_i$ is the ith canceling pulse, such that $\boldsymbol{c}_i \approx -\boldsymbol{f}_i$ in order to make $\boldsymbol{c} \approx -\boldsymbol{f}$.

Consider two clipping pulses, $\boldsymbol{f}_i$ and $\boldsymbol{f}_j$, having the same peak magnitude at some level, denoted as

$$\ell = \max |\boldsymbol{f}_i| \approx \max |\boldsymbol{f}_j|. \tag{35}$$

Because of the property of constant-phase near their maximum, the clipping pulses can be approximated by a cyclic shift with an appropriate amount of phase rotation:

$$\boldsymbol{f}_j \approx \mathrm{e}^{j\left(\angle f_j[\hat{n}_j] - \angle f_i[\hat{n}_i]\right)} \circlearrowright_{\hat{n}_j - \hat{n}_i} (\boldsymbol{f}_i), \tag{36}$$

where $f_i[\hat{n}_i]$ and $f_j[\hat{n}_j]$ are the samples of $\boldsymbol{f}_i$, and $\boldsymbol{f}_j$ having the maximum magnitudes, respectively. Equation (36) suggests that the canceling pulse for $\boldsymbol{f}_j$ can also be derived from the one used to cancel $\boldsymbol{f}_i$, that is:

$$\boldsymbol{c}_j \approx \mathrm{e}^{j\left(\angle f_j[\hat{n}_j] - \angle f_i[\hat{n}_i]\right)} \circlearrowright_{\hat{n}_j - \hat{n}_i} (\boldsymbol{c}_i). \tag{37}$$

Let $\boldsymbol{C}_i = [C_i[0], \ldots, C_i[NJ-1]]$ and $\boldsymbol{F}_i = [F_i[0], \ldots, F_i[NJ-1]]$, respectively, be the corresponding frequency vectors of $\boldsymbol{c}_i$ and $\boldsymbol{f}_i$ obtained from DFT operations. Then it follows from (36) that:

$$\begin{aligned} F_j[k] &= \mathcal{F}\{\boldsymbol{f}_j\}|_k; \quad (0 \le k \le NJ-1) \\ &\approx \mathrm{e}^{j\left(\angle f_j[\hat{n}_j] - \angle f_i[\hat{n}_i]\right)} \mathcal{F}\{\circlearrowright_{\hat{n}_j - \hat{n}_i} (\boldsymbol{f}_i)\}|_k \\ &\approx \mathrm{e}^{j\left(\angle f_j[\hat{n}_j] - \angle f_i[\hat{n}_i]\right)} \mathrm{e}^{-j2\pi(\hat{n}_j - \hat{n}_i)k/NJ} \mathcal{F}\{\boldsymbol{f}_i\}|_k \\ &\approx \mathrm{e}^{j\left(\angle f_j[\hat{n}_j] - \angle f_i[\hat{n}_i]\right)} \mathrm{e}^{-j2\pi(\hat{n}_j - \hat{n}_i)k/NJ} F_i[k]. \end{aligned} \tag{38}$$

Similarly, it follows from (37) that:

$$C_j[k] \approx \mathrm{e}^{j\left(\angle f_j[\hat{n}_j] - \angle f_i[\hat{n}_i]\right)} \mathrm{e}^{-j2\pi(\hat{n}_j - \hat{n}_i)k/NJ} C_i[k], \tag{39}$$

where $0 \le k \le NJ-1$. Thus, comparing (38) and (39) yields:

$$g_\ell[k] = \frac{C_j[k]}{F_j[k]} \approx \frac{C_i[k]}{F_i[k]}; \quad (0 \le k \le NJ-1). \tag{40}$$

Equation (40) implies that the ratios of the frequency components between the clipping pulses of the same peak magnitudes and their canceling pulses are approximately constant. For each level ℓ, these ratios are defined as a coefficient vector $\boldsymbol{g}_\ell = [g_\ell[0], \ldots, g_\ell[NJ-1]]$. Using such a coefficient vector, the canceling pulse of a clipping pulse $\tilde{\boldsymbol{f}}$ whose peak magnitude is at level ℓ can be obtained by:

$$\tilde{\boldsymbol{c}} = \mathcal{F}^{-1}\{\boldsymbol{g}_\ell \mathcal{F}\{\tilde{\boldsymbol{f}}\}\}. \tag{41}$$

Equation (41) can be used to construct a canceling pulse from the frequency vector of a clipping pulse and the corresponding coefficients. Based on the above analysis, the proposed clipping and filtering algorithm is performed in two stages. The first stage, also called a learning stage, initializes a set of coefficient vectors corresponding to different levels of clipping pulses. This stage can be done off-line and updated regularly when needed. The second stage is an online process that processes the clipping noise in the frequency domain with the suitable coefficients developed from the first stage to iteratively construct a peak canceling signal.

1) STAGE 1 – LEARNING

This stage has the same steps discussed in Section IV-A1. Specifically, the reference signals constructed as in (25) are clipped:

$$\hat{\boldsymbol{f}}_{\mathcal{T},i} = \hat{\boldsymbol{x}}_i - g_{\mathcal{T}}(\hat{\boldsymbol{x}}_i). \tag{42}$$

Then q coefficient vectors are calculated as:

$$\boldsymbol{g}_{\mathcal{T},i} = \frac{\mathcal{F}\{\hat{\boldsymbol{c}}_{\mathcal{T},i}\}}{\mathcal{F}\{\hat{\boldsymbol{f}}_{\mathcal{T},i}\}}, \tag{43}$$

where $\hat{\boldsymbol{c}}_{\mathcal{T},i}$ is given by (26).

The stage finishes by finding a set of coefficient vectors

$$\mathcal{G}_{\mathcal{T}} = \{\boldsymbol{g}_{\mathcal{T},0}, \ldots, \boldsymbol{g}_{\mathcal{T},q}\}. \tag{44}$$

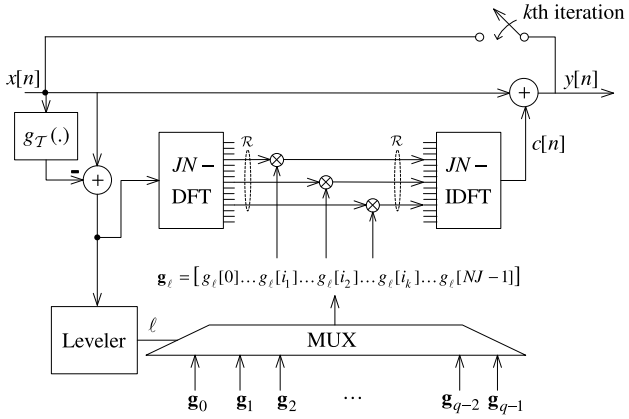

FIGURE 3. Hardware implementation structure for proposed CFTR algorithm.

2) STAGE 2 – Peak-Reduction LOOP

The second stage reduces the peak of each symbol iteratively. At the kth iteration, the clipping noise vector $\boldsymbol{f}_k = \boldsymbol{x} + \boldsymbol{c}_k - g_{\mathcal{T}}(\boldsymbol{x} + \boldsymbol{c}_k)$ is also approximated by P_k clipping pulses as in (28). For simplicity, only the clipping pulse of highest peak magnitude is selected

$$\tilde{\boldsymbol{f}}_k = \arg \max_{1 \le i \le P_k} |\boldsymbol{f}_{k,i}|. \tag{45}$$

The corresponding level of $\tilde{\boldsymbol{f}}_k$ is obtained as in (30). Then the canceling signal for the next iteration is:

$$\boldsymbol{c}_{k+1} = \mathcal{F}^{-1}\{\boldsymbol{g}_{\ell_k} \mathcal{F}\{\tilde{\boldsymbol{f}}_k\}\}. \tag{46}$$

The peak-reduction loop is illustrated in Fig. 3. The purpose of the leveler block in the figure is to conduct the operation in (30). All of the coefficient vectors calculated from the learning stage can be stored in a memory, and a multiplexer (MUX) structure is used to fetch a corresponding coefficient vector at run-time.

V. COMPLEXITY ANALYSIS

This section analyzes and compares the complexity of the conventional GTR and CFTR algorithms, as well as the two algorithms proposed in this paper.

First, the conventional GTR algorithm works with time domain samples and requires a large number of multiplications and additions per iteration. Specifically, the calculation of $\alpha_{k,i}$ needs $2|\mathcal{M}_k|$ real multiplications. The scaling with $\alpha_{k,i}$ and γ in (14) requires additional 4 $(|\mathcal{M}_k|JN + JN)$ real multiplications. Thus, in total, the number of multiplications per iteration of the GTR algorithm is $4|\mathcal{M}_k|JN + 2|\mathcal{M}_k| + 4JN$. The number of additions required by the GTR algorithm is $2|\mathcal{M}_k|JN + 2$ for each iteration, which is in the same order as the number of multiplications.

Moreover, it should be pointed out that γ is defined as a constant in [3], [4] and how to properly choose its value is not thoroughly studied in literature. A large value of γ could cause the algorithm fail to converge as the set $\mathcal{M}_k$ grows larger after each iteration. On the other hand, a small value of γ makes the algorithm converge slowly.

For our proposed GTR algorithm, a single iteration of the algorithm requires $4P_kJN$ real multiplications and $2P_kJN$ additions. Since $P_k \ll |\mathcal{M}_k|$, the number of multiplications and additions per iteration of the proposed algorithm are significantly less than the corresponding numbers of the GTR algorithm as discussed in Section III-A. Moreover, the proposed algorithm does not need to try different values of γ to obtain the optimal amount of peak reduction.

Note that the overall complexity grows with the number of iterations. Therefore reducing the number of iterations helps to reduce the cost of the PAPR reduction process. The proposed algorithm transfers most of the computational cost to off-line processing, which can be regularly updated upon changes in the frequency settings. As can be seen in Section VI, the additional step of precalculating the canceling signals makes the proposed algorithm converge in a smaller number of iterations as compared to the conventional GTR algorithm, thereby further reducing its computational cost.

Next, for the conventional CFTR method, the complexity comes mainly from the JN-point DFT/IDFT pair and the weighting of the canceling signal in (20). The former can be efficiently implemented by FFT/IFFT, which has a complexity of $\mathcal{O}(JN \log(JN))$. The latter needs $4|\mathcal{S}|$ real multiplications, one real division for the calculation of β in (22) and $2JN$ real multiplications to scale the time vector $\boldsymbol{c}$. In total, per iteration, the CFTR algorithm requires 1 real division and $(M_{\text{DFT}} + M_{\text{IDFT}} + 4|\mathcal{S}| + 2JN)$ multiplications, where $M_{\text{DFT}} = M_{\text{IDFT}} = JN \log_2(JN)$ is the number of multiplications performed by the DFT and IDFT blocks. Compared to the conventional GTR algorithm, the CFTR algorithm needs a lower number of iterations (as shown in Section VI) and has lower complexity. However, its complexity is still very high for practical hardware implementation.

On the other hand, the proposed CFTR algorithm reduces the computational complexity of the conventional CFTR algorithm. Specifically, thanks to the coefficients found in the learning stage, the online processing stage removes the need for calculating β and scaling the time-domain vector as in the conventional approach. In addition, the division operations are removed from the proposed scheme, and the number of multiplications per iteration is $M_{\text{DFT}} + M_{\text{IDFT}} + 4|\mathcal{R}| = JN \log_2(JN) + 4|\mathcal{R}|$, where $4|\mathcal{R}|$ multiplications are used to generate the canceling signal in (46). Since $|\mathcal{R}| \ll JN$, the complexity of the proposed clipping and filtering algorithm is much lower than that of the conventional CFTR algorithm (see Section III-B). As will be shown in Section VI, simulation results reveal that the performance of the proposed CFTR algorithm is comparable to that of the conventional CFTR algorithm.

Compared to the proposed GTR algorithm in Section IV-A, the proposed CFTR algorithm has fewer multiplications per iteration. In addition, the DFT/IDFT operations can be efficiently implemented using FFT/IFFT algorithms. Therefore the proposed CFTR algorithm is very attractive for practical applications.

TABLE 1. Complexity comparison of different PAPR reduction methods.

	Complexity per iteration
GTR	$2\left(\lvert\mathcal{M}_k\rvert JN + 2\lvert\mathcal{M}_k\rvert + 4JN\right)$
Proposed GTR	$4P_k JN + 2P_k JN$
CFTR	$2JN\log_2(JN) + 4\lvert\mathcal{S}\rvert + 2JN$
Proposed CFTR	$2JN\log_2(JN) + 4\lvert\mathcal{R}\rvert$

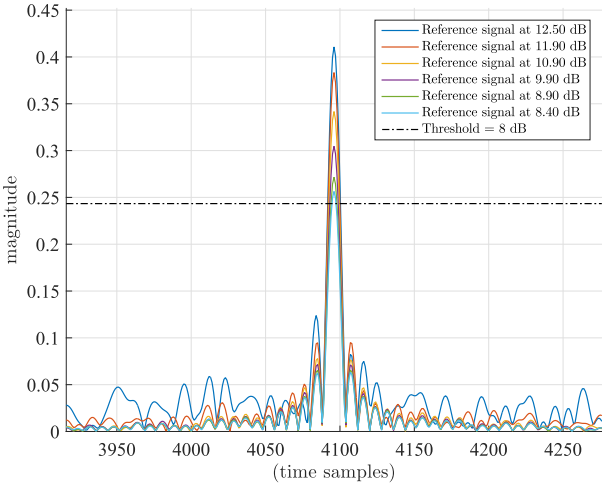

FIGURE 4. Example of reference signals with $G = 100$ reserved tones, and target PAPR of 8 dB (centered at index 4096).

In summary, the complexity of the conventional and proposed methods are summarized in Table. 1. It is worth noting that the learning stage of our proposed methods can be performed off-line, which means that its computational complexity can be justified. The significant complexity reduction of our proposed algorithms is in the online stage, which is performed for data transmission and reception of each and every OFDM symbol. Furthermore, not only do the proposed methods remarkably save computational resources, they also lower the latency caused by the PAPR reduction process.

VI. SIMULATION RESULTS

In this section, we consider an OFDM system employing 1024−QAM constellation and $N = 1024$ subcarriers as supported in DOCSIS 3.1 standard. The oversampling factor is chosen to be $J = 8$. In each simulation, 10^6 OFDM symbols are generated. Two different sets of reserved tones are simulated. In the first case, $G = 50$ tones, which is approximately 5% of the available tones, are selected randomly. Hence the number of data tones is $N - G = 1024 - 50 = 974$. The second case considers $G = 100$ tones, which are also randomly selected, and the corresponding number of data tones is $G = 1024 - 100 = 924$.

For each of these two cases, two different target PAPR levels and corresponding thresholds $\mathcal{T}$ are tested, namely 8 dB and 10 dB. The learning stage was run over 5×10^5 OFDM symbols. The quantization level $\delta_{\mathcal{T}}$ was set to provide a resolution of 0.1 dB. This means, for example, in the case of 8 dB threshold, $\mathcal{B}_0$ consists of signals with PAPR in the range [8 dB, 8.1 dB], $\mathcal{B}_1$ for the signals with PAPR

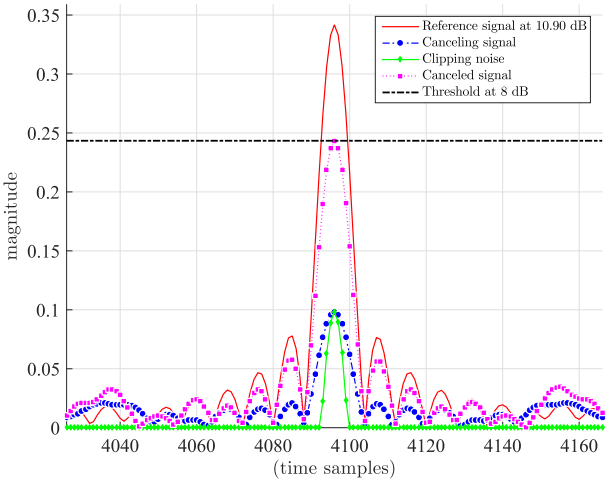

FIGURE 5. Example of a reference signal and its canceling signal with $G = 100$ reserved tones, and target PAPR of 8 dB (centered at index 4096).

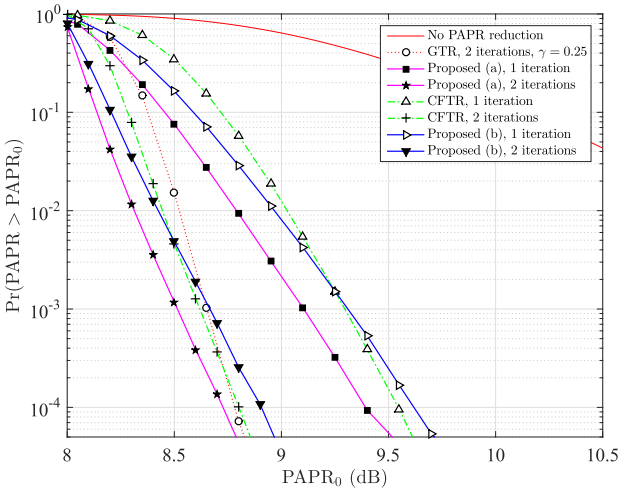

FIGURE 6. Comparison of PAPR reduction for different methods $G = 50$ random reserved tones with target PAPR, $\mathcal{T} = 8$ dB. "Proposed (a)" is for the proposed time-domain algorithm, "Proposed (b)" is for the proposed clipping and filtering algorithm.

in [8.1 dB, 8.2 dB] and so on. Extensive testing indicates that this value of $\delta_{\mathcal{T}}$ provides fine enough resolution for the reference signals.

Fig. 4 shows examples of reference signals of different peak levels. The levels are measured in dB with respect to the average magnitude of OFDM symbols. It is interesting to see that the main lobes of all reference signals have essentially the same width, while the side lobe levels are much smaller when compared to side-lobes of random OFDM signals.

Fig. 5 presents an example of a reference signal with a maximum magnitude of 10.9 dB, its clipping noise, the corresponding canceling signal and the canceled signal obtained by subtracting the canceling signal from the reference signal.

Figs. 6 and 7 compare the PAPR reduction performance of different algorithms with a target PAPR of 8 dB using 50 and 100 reserved tones, respectively. Similarly, Figs. 8 and 9 report results for a target PAPR of 10 dB. In all

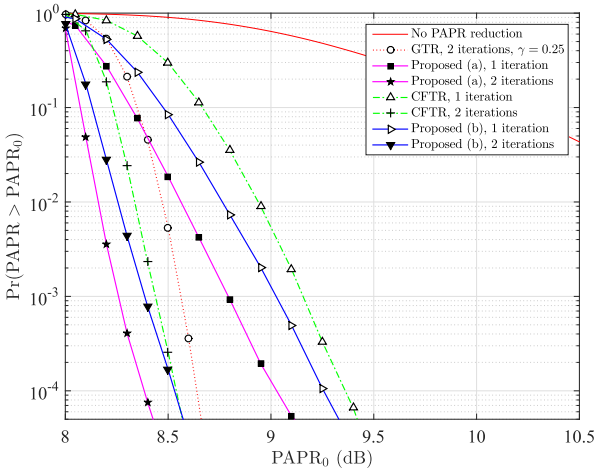

FIGURE 7. Comparison of PAPR reduction for different methods $G = 100$ random reserved tones with target PAPR, $\mathcal{T} = 8$ dB. "Proposed (a)" is for the proposed time-domain algorithm, "Proposed (b)" is for the proposed clipping and filtering algorithm.

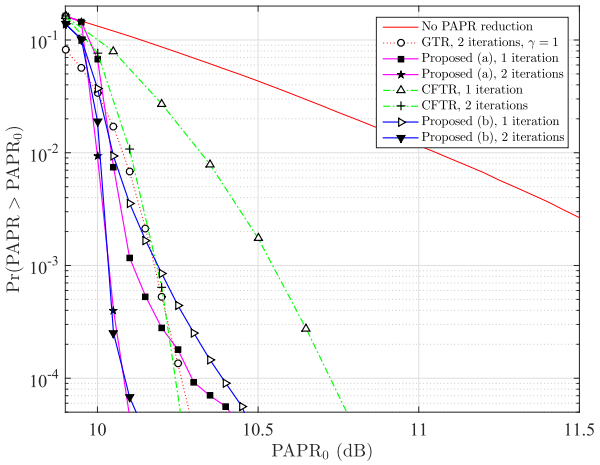

FIGURE 8. Comparison of PAPR reduction for different methods $G = 50$ random reserved tones with target PAPR, $\mathcal{T} = 10$ dB. "Proposed (a)" is for the proposed time-domain algorithm, "Proposed (b)" is for the proposed clipping and filtering algorithm.

cases, the CCDF curves with 1 iteration and 2 iterations of the proposed algorithms are compared against those of the conventional GTR and CFTR algorithms having the same number of iterations. For the conventional GTR algorithm, different values of scaling factor γ are tested: 0.01, 0.05, 0.1, 0.15, 0.2, 0.25, 0.5 and 1. The scaling factor yielding the best peak reduction performance after 2 iterations was selected and indicated in the figure's legend.

Figs. 6 to 9 show that for both $\mathcal{T} = 8$ dB and $\mathcal{T} = 10$ dB, the proposed algorithms generally provide slightly better peak reduction than the conventional algorithms. As expected, the results indicate that reserving more tones provides better PAPR reduction. Specifically, at $\mathcal{T} = 8$ dB and probability of 10^{-4}, doubling the number of reserved tones from 50 to 100 can increase the peak reduction performance by approximately 0.5 dB.

For the higher threshold of $\mathcal{T} = 10$ dB, the proposed algorithms can provide the same performance with one iteration as

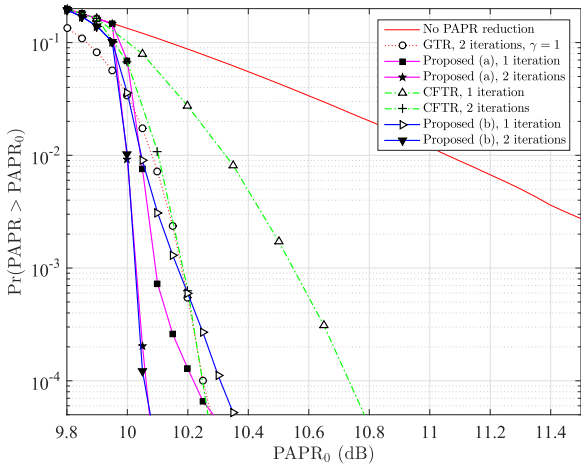

FIGURE 9. Comparison of PAPR reduction for different methods $G = 100$ random reserved tones with target PAPR, $\mathcal{T} = 10$ dB. "Proposed (a)" is for the proposed time-domain algorithm, "Proposed (b)" is for the proposed clipping and filtering algorithm.

the conventional algorithms achieve in two iterations, which is approximately 0.6 dB better than the conventional CFTR achieves in one iteration. Moreover, it should be pointed out that the computational complexity of the proposed algorithms, even when two iterations are used, is still much lower than that of the conventional GTR and CFTR algorithms.

VII. CONCLUSION

This paper presents two novel TR-based algorithms for peak reduction of OFDM signals: a time-domain algorithm and a clipping-and-filtering algorithm. Both algorithms efficiently reuse precalculated canceling signals to reduce the computational complexity of the conventional peak reduction algorithms based on the TR principle. The precalculated canceling signals can be updated when different tone sets are selected for data transmission, accommodating many practical applications. Both algorithms are distortionless, hence do not affect the BER performance of information bits sent on the data tones. Simulation results show that the proposed algorithms achieve slightly better PAPR performance than the conventional CFTR and GTR algorithms. Moreover, such performance is achieved with much lower computational complexity when compared to the conventional GTR and CFTR algorithms. Among all four algorithms considered, the proposed time-domain GTR algorithm gives the best peak reduction performance but the proposed clipping-and-filtering algorithm requires considerably fewer multiplications per iteration and can be efficiently implemented using FFT/IFFT structure.

REFERENCES

[1] Y. Rahmatallah and S. Mohan, "Peak-to-average power ratio reduction in OFDM systems: A survey and taxonomy," *IEEE Commun. Surveys Tuts.*, vol. 15, no. 4, pp. 1567–1592, Nov. 2013.

[2] R. Yoshizawa and H. Ochiai, "Effect of clipping and filtering with distortionless PAPR reduction for OFDM systems," in *Proc. Veh. Technol. Conf. (VTC Fall)*, 2015, Sep. 2015, pp. 1–5.

[3] J. Tellado and J. M. Cioffi, "Peak power reduction for multicarrier transmission," in *Proc. IEEE GLOBECOM*, vol. 99, Dec. 1999, pp. 5–9.

[4] J. Tellado, *Multicarrier Modulation With Low PAR: Applications to DSL and Wireless*, vol. 587. Cham, Switzerland: Springer, 2006.
[5] J.-C. Chen, M.-H. Chiu, Y.-S. Yang, and C.-P. Li, "A suboptimal tone reservation algorithm based on cross-entropy method for PAPR reduction in OFDM systems," *IEEE Trans. Broadcast.*, vol. 57, no. 3, pp. 752–756, Sep. 2011.
[6] J. Lv and Y. Wan, "An improved tone reservation method for PAPR reduction in OFDM systems," in *Proc. Int. Conf. Mech. Sci., Electr. Eng. Comput. (MEC)*, Dec. 2013, pp. 3791–3794.
[7] X. Lv and Y. Wan, "Efficient tone reservation peak-to-average power ratio reduction system with optimal clipping for orthogonal frequency division multiplexing systems," *IET Commun.*, vol. 9, no. 17, pp. 2070–2076, Nov. 2015.
[8] D. Guel and J. Palicot, "FFT/IFFT pair based digital filtering for the transformation of adding signal PAPR reduction techniques in tone reservation techniques," in *Proc. 5th Int. Conf. Wireless Mobile Commun.*, 2009, pp. 200–204.
[9] Y.-C. Wang and Z.-Q. Luo, "Optimized iterative clipping and filtering for PAPR reduction of OFDM signals," *IEEE Trans. Commun.*, vol. 59, no. 1, pp. 33–37, Jan. 2011.
[10] D. Guel and J. Palicot, "Transformation of any adding signal technique in tone reservation technique for PAPR mitigation thanks to frequency domain filtering," *Int. J. Adv. Telecommun.*, vol. 4, no. 1, pp. 213–225, 2011.
[11] Y. Wang, W. Chen, and C. Tellambura, "Genetic algorithm based nearly optimal peak reduction tone set selection for adaptive amplitude clipping PAPR reduction," *IEEE Trans. Broadcast.*, vol. 58, no. 3, pp. 462–471, Sep. 2012.
[12] J. Bai, Y. Li, W. Cheng, H. Du, and Y. Wang, "A novel peak-to-average power ratio reduction scheme via tone reservation in OFDM systems," *China Commun.*, vol. 14, no. 11, pp. 279–290, Nov. 2017.
[13] E. Tampubolon and H. Boche, "Probabilistic analysis of tone reservation method for the PAPR reduction of OFDM systems," in *Proc. IEEE Int. Conf. Acoust., Speech Signal Process. (ICASSP)*, Mar. 2017, pp. 3799–3803.
[14] H. Li, J. Wei, and N. Jin, "Low-complexity tone reservation scheme using pre-generated peak-canceling signals," *IEEE Commun. Lett.*, vol. 23, no. 9, pp. 1586–1589, Sep. 2019.
[15] X. Liu, X. Zhang, J. Xiong, and J. Wei, "An enhanced iterative clipping and filtering method using time-domain kernel matrix for PAPR reduction in OFDM systems," *IEEE Access*, vol. 7, pp. 59466–59476, 2019.
[16] Y. Wang, R. Zhang, J. Li, and F. Shu, "PAPR reduction based on parallel tabu search for tone reservation in OFDM systems," *IEEE Wireless Commun. Lett.*, vol. 8, no. 2, pp. 576–579, Apr. 2019.
[17] L. Wang and C. Tellambura, "Analysis of clipping noise and tone-reservation algorithms for peak reduction in OFDM systems," *IEEE Trans. Veh. Technol.*, vol. 57, no. 3, pp. 1675–1694, May 2008.
[18] C. Tellambura, "Computation of the continuous-time PAR of an OFDM signal with BPSK subcarriers," *IEEE Commun. Lett.*, vol. 5, no. 5, pp. 185–187, May 2001.
[19] S. Boyd and L. Vandenberghe, *Convex Optimization*. Cambridge, U.K.: Cambridge Univ. Press, 2004.
[20] Q. Nguyen, "Peak-to-average power ratio reduction of DOCSIS 3.1 downstream signals," M.Sc. thesis, Dept. Elect. Comput. Eng., Univ. Saskatchewan, Saskatoon, SK, Canada, Sep. 2018.

QUANG NGUYEN received the B.E. degree in computer engineering from the Hanoi University of Science and Technology, Hanoi, Vietnam, in 2011, and the M.Sc. degree in electrical engineering from the University of Saskatchewan, SK, Canada, in 2018. He joined SED Systems, a Division of Calian Ltd., for eight months working with a VHDL-based design for remote PHY. In 2019, he relocated to Ottawa and joined Ross Video as an FPGA Hardware Designer. He has been working with the next generation of video routers for live television, news, sports, and entertainment. His active working areas involve designing FPGA with 12G and 25G transceivers, signal integrity simulation and analysis, and bringing up boards.

THE KHAI NGUYEN received the B.Eng. degree from the School of Electronics and Telecommunications, Hanoi University of Science and Technology, Vietnam, in 2017, and the M.Sc. degree in electrical engineering from the University of Saskatchewan, in 2020, where he is currently pursuing the Ph.D. degree. His research interests include wireless communications, channel coding, and signal processing for broadband systems.

HA H. NGUYEN (Senior Member, IEEE) received the bachelor's degree in electrical engineering from the Hanoi University of Technology (HUT), Hanoi, Vietnam, in 1995, the master's degree in electrical engineering from the Asian Institute of Technology (AIT), Bangkok, Thailand, in 1997, and the Ph.D. degree in electrical engineering from the University of Manitoba, Winnipeg, MB, Canada, in 2001. He joined the Department of Electrical and Computer Engineering, University of Saskatchewan, Saskatoon, SK, Canada, in 2001, and became a Full Professor, in 2007. He is currently the NSERC/Cisco Industrial Research Chair of Low-Power Wireless Access for Sensor Networks. He is the coauthor, with Ed Shwedyk, of the textbook *A First Course in Digital Communications* (Cambridge University Press). His research interests include the areas of communication theory, wireless communications, and statistical signal processing. He is a fellow of the Engineering Institute of Canada (EIC) and a Registered Member of the Association of Professional Engineers and Geoscientists of Saskatchewan (APEGS). He was an Associate Editor of the IEEE TRANSACTIONS ON WIRELESS COMMUNICATIONS and IEEE WIRELESS COMMUNICATIONS LETTERS, from 2007 to 2011 and from 2011 to 2016, respectively. He is currently serving as an Associate Editor for the IEEE TRANSACTIONS ON VEHICULAR TECHNOLOGY and IEEE TRANSACTIONS ON COMMUNICATIONS. He served as a technical program chair for numerous IEEE events. He was the General Chair of the 30th Biennial Symposium on Communications, in 2021.

BRIAN BERSCHEID (Member, IEEE) received the B.E. and Ph.D. degrees in electrical engineering from the University of Saskatchewan, Saskatoon, SK, Canada, in 2006 and 2011, respectively. From 2006 to 2017, he was with Vecima Networks, where he designed broadband cable access equipment and researched next-generation access technologies. In 2017, he joined the Department of Electrical and Computer Engineering, University of Saskatchewan, as the Barbhold Chair in information technology and an Assistant Professor. He is currently licensed as a Professional Engineer with the Association of Professional Engineers and Geoscientists of Saskatchewan. His research interests include the design and implementation of algorithms for communications, signal processing, and machine learning.